Rapamycin induces growth retardation by disrupting angiogenesis in the growth plate

Óscar Álvarez-García[1], Enrique García-López[2], Vanessa Loredo[1], Helena Gil-Peña[1], Julián Rodríguez-Suárez[1], Flor Á. Ordóñez[1], Eduardo Carbajo-Pérez[3] and Fernando Santos[1,3]

[1]Department of Pediatrics, Hospital Universitario Central de Asturias, Oviedo, Spain; [2]Department of Pediatrics, Hospital Álvarez-Buylla, Oviedo, Spain and [3]Department of Medicine, Universidad de Oviedo, Oviedo, Spain

Rapamycin, a potent immunosuppressant used in renal transplantation, has been reported to impair longitudinal growth in experimental studies. Rapamycin is both antiproliferative and antiangiogenic; therefore, it has the potential to disrupt vascular endothelial growth factor (VEGF) action in the growth plate and to interfere with insulin-like growth factor I (IGF-I) signaling. To further investigate the mechanisms of rapamycin action on longitudinal growth, we gave the 4-week-old rats rapamycin daily for two weeks. Compared with a vehicle-treated group, rapamycin-treated animals were severely growth retarded and had marked alterations in the growth plate. Vascular invasion was disturbed in the rapamycin group, there was a significant reduction in osteoclast cells near the chondro-osseus junction, and there was lower VEGF protein and mRNA expression in the terminal chondrocytes of the growth cartilage. Compared with the control group, the rapamycin group had higher levels of circulating IGF-I as well as the mRNAs for IGF-I and of the receptors of IGF-I and growth hormone in the liver but not in the growth cartilage. Thus our findings explain the adverse effect of rapamycin on growth plate dynamics. This should be taken into account when the drug is administered to children.

Kidney International (2010) **78,** 561–568; doi:10.1038/ki.2010.173; published online 16 June 2010

KEYWORDS: children; pediatric kidney transplantation; transplantation; vascular endothelial growth factor

Correspondence: *Fernando Santos, Pediatria, Facultad de Medicina, Hospital Universitario Central de Asturias, C/Julian Claveria 6, Oviedo 33006, Spain. E-mail: fsantos@uniovi.es*

Received 22 December 2009; revised 30 March 2010; accepted 21 April 2010; published online 16 June 2010

Rapamycin (Rapamune, Wyeth Pharmaceuticals, Philadelphia, PA, USA) has been widely used as an immunosuppressant for the treatment of renal transplanted patients.[1] Early studies reported that rapamycin (LC Laboratories, Woburn, MA, USA), alone or in combination with calcineurin inhibitors, improved renal function[2,3] and decreased the risk of developing tumors in transplanted patients.[4,5] In addition, mammalian target of rapamycin (mTOR) inhibitors, such as rapamycin and its derivatives (rapalogs), proved to be effective against various proliferative disorders[6–8] mainly because they exhibit both antiproliferative[9] and antiangiogenic[10] activities. However, rapamycin therapy should be restricted to very particular conditions because of the risk of severe side effects, including increases in serum cholesterol and triglycerides, anemia, proteinuria, skin rashes, and diarrhea.[11]

In pediatric patients, rapamycin is mainly used as a substitute for calcineurin inhibitors when nephrotoxicity or proliferative diseases occur.[12] One of the main challenges in the management of children with chronic disorders is to preserve the linear growth and rapamycin has the potential to interfere with longitudinal growth. Recent studies have shown that rapamycin administration impairs longitudinal growth in fast-growing rats,[13,14] and local infusion of rapamycin directly into the proximal tibial growth plates of rabbits has also been shown to inhibit overall long bone growth.[15] Longitudinal growth is the result of new bone formation during endochondral ossification, in which proliferation and differentiation of epiphyseal growth plate chondrocytes directly correlate with bone elongation. We[13] and others[14,15] have reported the adverse effects on chondrocyte proliferation and maturation in rapamycin-treated animals, which eventually resulted in a reduction of longitudinal growth velocity.

mTOR is a major regulator of cell growth and energetic metabolism,[16] acting downstream of growth factors as insulin and insulin-like growth factors (IGFs).[9] mTOR inhibition by rapamycin has been reported to partially block IGF-I intracellular signaling and its subsequent effects.[17–19] Besides growth hormone (GH), IGF-I has a key role in bone elongation, and both systemic and local alterations of GH–IGF-I axis are associated with severe growth

retardation.[20] Therefore, inhibition of IGF-I signaling by rapamycin could affect longitudinal growth, however, this hypothesis has not been so far addressed.

Vascular invasion of the growth cartilage is another essential process for physiological bone formation during endochondral ossification. Vascular endothelial growth factor A (VEGF) has a key role in the vascular invasion of the growth cartilage, and its inactivation results in a considerable expansion of the hypertrophic zone of the growth plate and disrupts the normal vascular pattern of the growth plate in young mice.[21] Guba *et al.*[10] reported that in tumoral tissues, the antiangiogenic activity of rapamycin was linked to a decrease in VEGF production and to an inhibited response of vascular endothelial cells to VEGF stimulation. Additional experimental evidence support the adverse effect of rapamycin on VEGF, not only on mRNA synthesis,[22] but also on protein production and secretion.[23–25] The tibial growth plate of rats with growth retardation induced by rapamycin exhibit morphological abnormalities indicative of severe disturbance of the vascular invasion process as well as expansion of the hypertrophic zone, similar to that observed in VEGF inactivated mice, and decreased VEGF immunohistochemical signal.[13,14,21]

Although there are strong experimental evidence that rapamycin impairs longitudinal growth, its mechanisms of action remain to be elucidated. On the basis of the hypothesis that rapamycin can interfere with IGF-I signaling and disrupt VEGF activity in the growth plate, the study presented here was carried out to further investigate the mechanisms of rapamycin actions on longitudinal growth by using an experimental young rat model.

RESULTS

Growth and nutrition

Rapamycin trough levels in rapamycin-treated animals (RAPA) group were 20.2 ± 1.5 ng/ml. Table 1 shows that administration of rapamycin exerted a marked adverse effect on longitudinal growth, as showed by significant reductions in nose to tail-tip length gain and longitudinal bone growth rate of RAPA rats in comparison with control animals. No changes in weight gain, food intake, and food efficiency were observed between the two groups.

Growth plate analysis

Epiphyseal cartilages of rapamycin-treated animals exhibited marked alterations in proliferative and hypertrophic zones. Bromodeoxyuridine (BrdU)-labeled chondrocytes were localized in the proliferative zones of both groups and the percentage of labeled nuclei was significantly ($P \leqslant 0.05$) higher in C (40.6 ± 1.3%) than in RAPA (32.2 ± 1.6%) group. Histomorphometric analysis revealed differences in the height of the epiphyseal cartilage, which was much higher in RAPA group than in control animals (Table 2). These differences were also observed in the height of the hypertrophic zone. In addition, the height of terminal chondrocytes was significantly lower in RAPA than in C animals. No differences were found in the expression of collagen type X mRNA (Figure 1a) and protein (Figure 1b), and in alkaline phosphatase (Figure 1c).

Table 1 | Growth and food intake of control rats (C) and rats treated with rapamycin (RAPA)

	C (*n*=10)	RAPA (*n*=10)
Weight gain (g)	51.4 ± 2.3	49.9 ± 2.2
Change in length (cm)	6.2 ± 0.2	5.2 ± 0.2[a]
Longitudinal growth rate (μm/day)	185 ± 8	81 ± 5[a]
Cumulative food intake (g)	215.8 ± 6.4	217.9 ± 6.8
Food efficiency (g/g)	0.24 ± 0.01	0.23 ± 0.01

Values are expressed as mean ± s.e.m. Food efficiency was calculated as grams of gained weight divided by grams of consumed food.
[a]Means statistically different from C group ($P \leqslant 0.05$).

Table 2 | Characteristics of the growth plate of control rats (C) and rats treated with rapamycin (RAPA)

	C (*n*=10)	RAPA (*n*=10)
Epiphyseal cartilage height (μm)	395 ± 20	676 ± 35[a]
Hypertrophic zone height (μm)	246 ± 14	453 ± 17[a]
Height of terminal chondrocytes (μm)	30 ± 0	27 ± 0[a]

Values are expressed as mean ± s.e.m.
[a]Means statistically different from C group ($P \leqslant 0.05$).

Vascular invasion and VEGF expression

Picrosirius red/alcian blue/hematoxilin staining revealed morphological and structural differences in the vascular invasion front between both rats' groups. Whereas longitudinal septa of C animals were well defined and parallel to the long axis of the bone, RAPA animals exhibited a disturbed pattern with many transverse unresorbed septa and sinuous capillary sprouts (images not shown).

Tartrate-resistant acid phosphatase $(TRAP)^+$ cells were found in the primary spongiosa and along the vascular invasion front in all groups. In the area between the chondro-osseous junction and 50 μm deep in the primary spongiosa, the number of TRAP-reactive cells per mm^2 in RAPA samples (198 ± 19 $TRAP^+$ cells/mm^2) was significantly less than that in C (356 ± 11 $TRAP^+$ cells/mm^2). These differences were not observed in the zone farther than 50 μm of the cartilage distal end (C: 323 ± 8 $TRAP^+$ cells/mm^2; RAPA: 335 ± 25 $TRAP^+$ positive cells/mm^2).

VEGF immunohistochemical signal was localized within the cytoplasm of hypertrophic chondrocytes from the early hypertrophic zone to the distal end of the cartilage in C rats (Figure 2b), whereas the terminal chondrocytes were rarely immunopositive in rapamycin-treated animals (C: 78 ± 4 positive cells/100 terminal chondrocytes vs RAPA: 10 ± 1 positive cells/100 terminal chondrocytes). This pattern of VEGF protein distribution was also observed at mRNA level as disclosed by *in situ* hybridization experiments (Figure 2a).

No statistical differences were found for VEGF mRNA levels (Figure 3a) or protein (Figure 4a) between C and RAPA animals in the growth plate or in the kidney, and similar hipoxia-inducible factor 1α (HIF1α) mRNA levels were also found in both groups (Figure 3a).

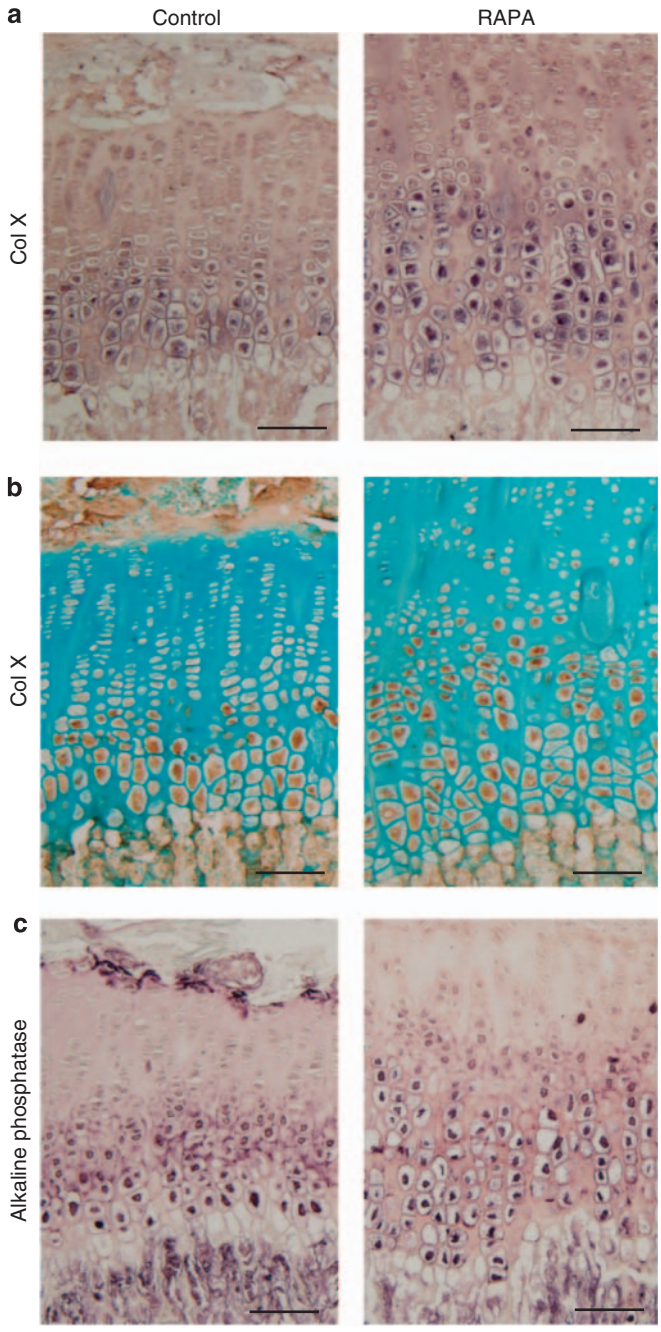

Figure 1 | Collagen X (Col X) expression and alkaline phosphatase in the growth cartilage of control and rapamycin-treated rats (RAPA). Representative images of *in situ* hybridization (**a**) and immunohistochemistry (**b**) of collagen X and alkaline phosphatase stain (**c**) are shown. Bar = 100 μm.

GH–IGF-I axis

Circulating levels of IGF-I were significantly greater in RAPA (680.7 ± 78.4 ng/ml) than in C (517.4 ± 41.1 ng/ml) animals. Rapamycin significantly upregulated hepatic mRNA levels of IGF-I, IGF-I receptor (IGF-IR), and GH receptor (GHR), as shown in Figure 3b. Interestingly, no significant differences in IGF-I, IGF-IR, and GHR mRNA levels were observed in the growth cartilage. As shown in Figures 2c, e and g, *in situ* hybridization signals for IGF-I, IGF-IR, and GHR, albeit more intense in early hypertrophic zone, were localized in the cytoplasm of nearly all hypertrophic chondrocytes of both groups of rats. Similar results were observed in the immunohistochemistry experiments for IGF-I and IGF-IR (Figures 2d and f). Insulin-like growth factor binding protein (IGFBP)-3 and IGFBP-5 immunohistochemical signal in growth cartilage was confined to hypertrophic chondrocytes and there were no differences between groups (Figure 5).

Autophagy

Autophagy was detected in liver and growth cartilage by the presence of microtubule-associated protein light chain 3 (LC3-II) isoform (Figure 4b). Rapamycin treatment did not increase autophagy in epiphyseal chondrocytes, whereas a consistent increase in LC3-II/LC3-I ratio was seen in the liver of RAPA animals, indicating an induction of the autophagic activity in this organ.

DISCUSSION

This study confirms that administration of rapamycin at doses that produce trough-circulating levels in the upper range of immunosuppressive concentrations used in renal transplantation, severely impairs the longitudinal growth rate. This undesirable effect should be taken into account when the drug is given to children and needs to be assessed in pediatric clinical series. The study provides novel information on the underlying mechanisms of growth retardation associated with rapamycin administration. VEGF was abnormally expressed in the growth cartilage of rapamycin-treated rats as VEGF mRNA and peptide signals were markedly reduced in the terminal chondrocytes sited adjacent to the primary spongiosa. In agreement with this finding and with the demonstrated role of VEGF as a key regulating factor of vascular invasion of the growth plate,[21] blood vessels and septa architecture within the primary spongiosa were profoundly disturbed by rapamycin administration. VEGF suppression has been reported to delay osteoclast recruitment and differentiation in the growth plate,[21] which is also consistent with the decreased number of $TRAP^+$ cells found in the cartilage-bone junction of rats receiving rapamycin. It is noteworthy that these alterations were found in the presence of unmodified total levels of growth plate VEGF and its mRNA, as measured by western blot and real time PCR, respectively, disclosing the critical importance of specific VEGF expression in the terminal differentiated chondrocytes for the normal regulation of the endochondral ossification process. The treatment with rapamycin, the way it was administered in our experimental model, did not impair the overall expression of VEGF and VEGF mRNA in the kidney. These findings are consistent with the lack of alterations found in the rapamycin-treated rats' mRNA levels of kidney and growth plate HIF-1α, peptide that has been reported to be a major regulator of VEGF expression;[26] however, it is in contrast with former studies showing VEGF downregulation by rapamycin in cultures of tumoral or overexpressing VEGF cells[22,23] and in

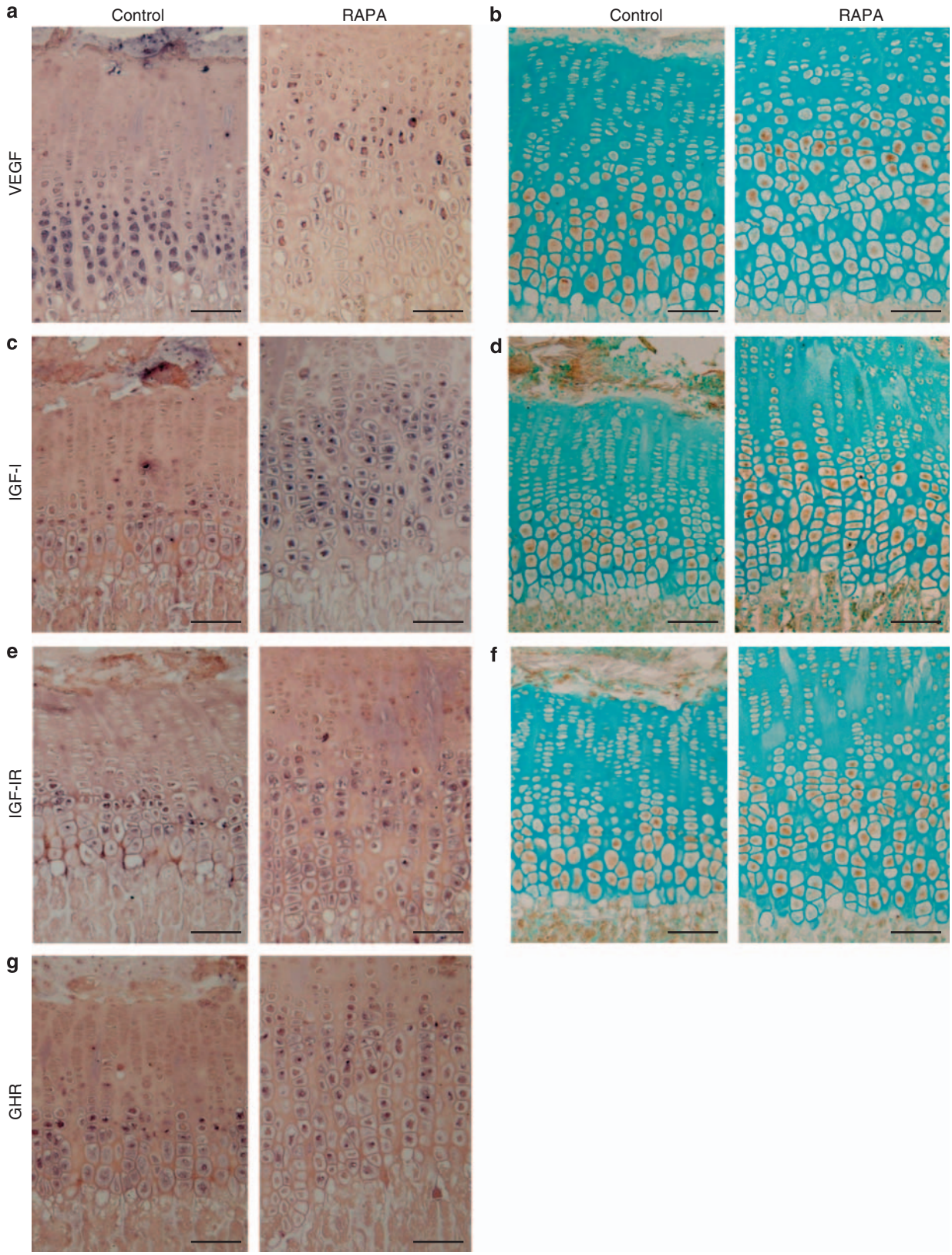

Figure 2 | *In situ* hybridization and immunohistochemistry analysis in the growth cartilage of proximal tibiae of control and rapamycin-treated rats (RAPA). Representative images of *in situ* hybridization experiments for vascular endothelial growth factor (VEGF) (**a**), insulin-like growth factor I (IGF-I) (**c**), IGF-I receptor (IGF-IR) (**e**), and growth hormone receptor (GHR) (**g**) mRNAs, and of immunohistochemistry experiments for VEGF (**b**), IGF-I (**d**), and IGF-IR (**f**) are shown. Bar = 100 μm.

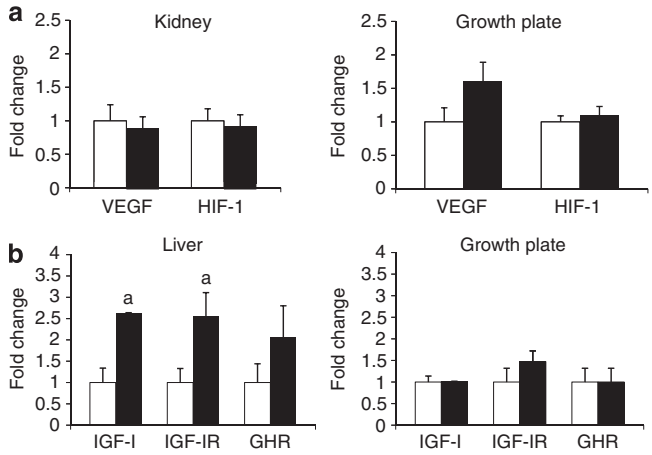

Figure 3 | Quantitative PCR experiments. (**a**) mRNA expression of vascular endothelial growth factor (VEGF) and HIF1α, in the whole kidney and the growth plate of control rats (white columns) and rats treated with rapamycin (black columns). (**b**) mRNA expression of insulin-like growth factor I (IGF-I), IGF-I receptor (IGF-IR), and growth hormone receptor (GHR) in the liver and the growth plate of control rats (white columns) and rats treated with rapamycin (black columns). Values are expressed as mean ± s.e.m. of gene fold-change relative to control group and normalized by glyceraldehyde 3-phosphate expression levels. [a]Means statistically different from C group ($P \leqslant 0.05$).

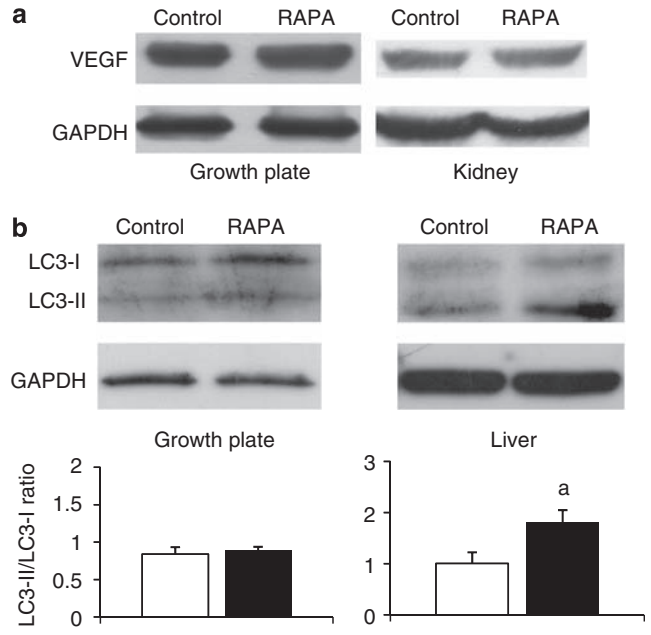

Figure 4 | Western blot experiments. (**a**) Analysis of vascular endothelial growth factor (VEGF) in the growth cartilage and kidney of control and rapamycin-treated rats (RAPA). (**b**) Analysis of LC3-I (18 kDa) and LC3-II (16 kDa) in the growth cartilage and liver of control (white columns) and rapamycin-treated rats (RAPA, black columns). Data are representative of three blots giving similar results. [a]Means statistically different from control group ($P \leqslant 0.05$). GAPDH, glyceraldehyde-3-phosphate dehydrogenase.

in vivo models treated with high doses of rapamycin.[10,25] This disparity may be related to different experimental conditions, dosage, and ways of rapamycin administration.

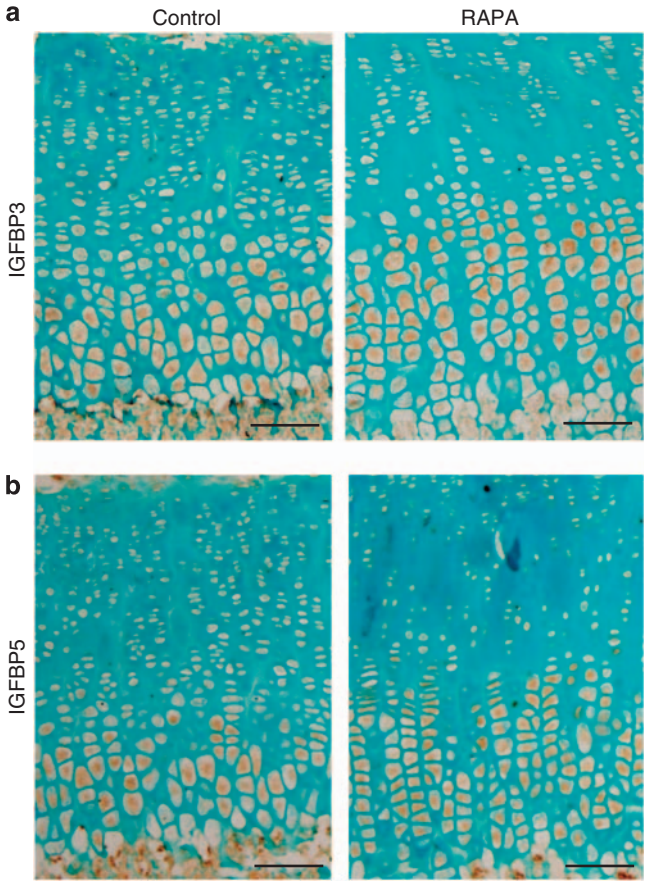

Figure 5 | Immunohistochemistry analysis of insulin-like growth factor binding proteins (IGFBPs) in the growth cartilage of proximal tibiae of control and rapamycin-treated rats (RAPA). Representative images of immunohistochemistry experiments for IGFBP-3 (**a**) and IGFBP-5 (**b**) are shown. Bar = 100 μm.

The present study also analyzed the effect of rapamycin administration on the GH–IGF-I axis, a major hormonal regulator of longitudinal growth. Circulating IGF-I concentrations were significantly higher in rapamycin-treated rats, likely as a result of increased hepatic IGF-I synthesis, as IGF-I mRNA was upregulated in this group of rats. It is noteworthy that a positive correlation between body size and circulating IGF-I levels has formerly been reported.[27] In spite of having higher concentrations of circulating IGF-I, rats treated with rapamycin grew less than their controls, indicating a potential resistance to the systemic action of IGF-I. This might result from mTOR inhibition by rapamycin, as mTOR has been reported to function downstream of IGFI receptor in the IGF-I signaling pathway.[9,16] It is interesting to point out that the rapamycin's effects were tissue dependent and the drug did not modify the local expression of IGF-I, IGF-IR, and GHR mRNAs in the growth plate. As IGFBP-3 and IGFBP-5 have been shown to inhibit and stimulate IGF-I action, respectively, in cultured rat growth plate chondrocytes,[28] immunohistochemical expression of these peptides was analyzed in the growth plate of untreated and rapamycin-treated rats without appreciating any difference. Thus, the

present study indicates that the adverse influence of rapamycin on longitudinal growth rate and on the proliferation and maturation of chondrocytes cannot be explained by interference with the local expression or activity of GH–IGF-I in the growth plate. It rather suggests that rapamycin itself was able to disturb the normal metabolism of the growth cartilage chondrocytes and, subsequently, slow down the longitudinal growth of treated individuals. In this regard, Bohensky *et al.*[29] have recently reported that mTOR inhibition induces autophagy in cultured chondrocytes. As autophagy is known to have a key role in chondrocyte survival and function within the growth plate,[30] it could be argued that the alterations in chondrocyte maturation and hypertrophy found in our rapamycin-treated animals were due to an enhanced autophagic process. The western blot analysis in the growth plate of LC3 (MBL International, Woburn, MA, USA) expression, a well known marker of autophagy, does not support this hypothesis and suggests again that the response to rapamycin is somewhat tissue specific (Figure 4b). Recent findings[31] have shown that in response to differential cues from mTOR, Notch serves as a molecular switch to couple two seemingly unrelated cellular processes: proliferation and differentiation. Interference of this signaling mTOR/Notch pathway by rapamycin might explain its effects on proliferation and differentiation of growth plate chondrocytes.

In summary, this study shows the adverse effect of rapamycin on growth and suggests for the first time that, in association with this undesirable effect, the drug disturbs the life cycle of growth plate chondrocytes, decreases the expression of VEGF in the growth cartilage adjacent to the methaphyseal bone, alters the process of vascular front invasion, and causes a state of resistance to endogenous IGF-I action.

ANIMALS AND METHODS

Male Sprague–Dawley rats aged 4 weeks and weighing 70 ± 5 g were housed in individual cages under controlled conditions of light (12 h light/dark cycle) and temperature (21–23°C). All animals received standard rat chow (A03; Panlab, Barcelona, Spain) and tap water. The study complied with current legislation on animal experiments in the European Union was approved by the Ethics Committee on Animal Research of the University of Oviedo, Spain.

Experimental protocol and sample collection

After 4 days of acclimation, animals were classified into two groups of 10 individuals each: RAPA and control animals pair-fed with RAPA group (C). From day 0 to day 13 of the protocol, 1 mg/kg/day of rapamycin diluted in 5% dimethyl sulfoxide (Sigma, St Louis, MO, USA) was administered intraperitoneally at 1000 hours to the RAPA group, whereas C group received vehicle (5% dimethyl sulfoxide). Animals were killed under anesthesia on day 14 of the protocol, approximately at the time of daily rapamycin injection. At 3 days before killing, each animal received 20 mg/kg of calcein (Sigma) by intraperitoneal route for calculation of osseous front advance as an index of longitudinal bone growth rate.[13] BrdU (100 mg/kg; Sigma) was also injected intraperitoneally at 1, 9, and 17 h before animals' death. Blood samples were collected and stored at −20°C until the measurement of rapamycin and circulating IGF-I concentrations. The whole left kidney, a portion of liver, and the proximal end of right tibiae were immediately frozen in liquid nitrogen for mRNA and protein studies. Proximal ends of left tibiae were embedded in methyl metacrilate as previously described.[32] Samples from half the animals were fixed in 40% ethanol and used for analysis of calcein and BrdU staining. The remaining samples were fixed in 4% paraformaldehyde and used for histomorphometry, immunohistochemistry, and *in situ* hybridization studies.

Blood measures

Trough concentrations of rapamycin were measured in whole-blood samples using an Abbott Imx analyzer (Abbott Cientifica, Madrid, Spain) as previously described.[13] IGF-I serum concentrations were measured by enzyme-linked immunosorbent assay using a commercial kit (Immunodiagnostic Systems, Boldon, UK). Inter- and intra-assay variation coefficients were under 7%.

Growth and nutrition

Food intake and body weight were measured daily using an electronic balance (Ohaus GT 2100, Florham Park, NJ, USA). Nose to tail-tip length was measured under anesthesia on days 0 and 14. Food efficiency was calculated as the ratio between weight gained and food consumed (g/g) by each animal between days 0 and 14 of the protocol. Longitudinal growth rate was measured in 10 µm-thick frontal sections of the proximal end of tibiae as described elsewhere.[32]

Growth plate histology and histomorphometry

Frontal sections (5 µm thick) of proximal tibiae fixed in formalin were stained by the following methods: alcian blue/safranine (Merck, Darmstadt, Germany) for morphometric analysis, alkaline phosphatase stain (Roche, Basel, Switzerland) for chondrocyte maturation, TRAP stain (Sigma) for osteoclast identification, and picrosirius red/alcian blue/hematoxylin (Merck) for analysis of bone and cartilage extracellular matrix. Heights of the growth cartilage and its hypertrophic zone were identified following morphological criteria and measured at regular intervals using an image analysis system described elsewhere.[13] Height of the three most distal hypertrophic chondrocytes was measured in alternate columns using the same system. The number of $TRAP^+$ cells at the vascular invasion front was measured in two different zones: an area extending 50 µm from the distal end of the growth cartilage into the primary spongiosa, and another area immediately below extending from 50 to 150 µm of the chondro-osseus union. Two slides per animal were used and results were expressed as the number of positive cells per mm^2.

Growth plate immunohistochemistry and *in situ* hybridization

Immunodetection of BrdU, IGF-I, IGF-IR, IGFBP-3, IGFBP-5, and VEGF were carried out as described elsewhere.[32,33] Two sections per animal were analyzed. The proliferating activity was expressed as the number of positive cells per 100 cells in the proliferative zone, previously defined as the band of tissue between the resting zone and a line traced by the most distal BrdU-labeled cells. VEGF immunohistochemical signal was measured in the three most distal chondrocytes and expressed as number of positive cells per 100 terminal chondrocytes.

In situ hybridization was used to define the mRNA distribution pattern of VEGF, collagen type X, IGF-I, IGF-R and GHR in the growth cartilage following a methodology previously described.[33] RNA probes were supplied by GeneDetect (Auckland, New Zealand). One section per animal was hybridized with a labeled sense riboprobe and a second section was incubated adding a negative control probe to the hybridization mixture. Two sections served as negative controls.

Real-time PCR

mRNA was extracted from frozen liver, kidney, and tibiae samples using a modified Chomczynski method.[34] Samples were diluted to 1 μmol/l per μl concentration before retrotranscription with a commercial kit (Qiagen Iberia, Madrid, Spain). RNA purity was assessed by 260/280 ratio measurement using a ultraviolet spectrophotometer (GeneQuant Pro, Amersham Biosciences, GE Healthcare Spain, Barcelona, Spain). VEGF, HIF1α, IGF-I, IGF-R, and GHR expression was quantified by real-time PCR on a sequence detection system step one (Applied Biosystems, Foster City, CA, USA) with SYBR Green (ABgene Products, Thermo Fisher Scientific, Rockford, IL, USA) as fluorophore and glyceraldehyde 3-phosphate as a housekeeping gene. Oligonucleotide primer pairs were as follows: for VEGF forward CGTCCAATTGAGACCATGGT and reverse TCCGCATGATCTGCATAGTGA; for IGF-I forward TACCAGCTCGGCCACAGC and reverse GTGGGCTT GTTGAAGTAAAAGC; for IGF-R forward GCTGCTGGACC ACAAATCG and reverse TCGCTTCCCACACACACTTG; and for GHR forward AATTAATCCAAGCCTGAGGGAAA and reverse GGAACGACACTTGGTGAATCG. Primer sequences were designed with the Prime Express software (Perkin-Elmer Applied Biosystems) and synthesized by Invitrogen (Fisher–Invitrogen, Barcelona, Spain) whereas glyceraldehyde 3-phosphate and HIF1α primers were synthesized and supplied by Qiagen (Qiagen Iberia).

Western blot

Frozen kidney, liver, and tibia samples were homogenized in a lysis buffer containing 1 M Tris pH 7.4, 0.1% Triton X-100, 500 mM EDTA, 300 mM saccharose, and a protease inhibitor tablet (Sigma). The cytosolic fraction was collected as a supernatant after centrifugation at 12,000 *g* for 10 min at 4°C. A total of 50 μg of protein were resolved in 4–20% sodium dodecyl sulfate–polyacrylamide gel electrophoresis and transferred to polyvinylidene difluoride membrane (Immobilon-P; Millipore Iberica, Madrid, Spain). The membranes were blocked in 5% (w/v) non-fat dry milk in TBST (Tris-buffered saline, pH 7.4, containing 0.05% Tween 20) at room temperature for 1 h. After blocking, blots were incubated with primary rabbit antibody specific to VEGF (Neo Markers, Westinghouse, CA, USA) or LC3 diluted 1:500 in TBST at 4°C overnight. Immunoblots were washed three times with TBST and incubated at room temperature for 1 h with the secondary antibody (En Vision; Dako Diagnosticos SA, Barcelona, Spain) diluted 1:5000 in TBST. Peroxidase activity was visualized using a chemiluminescent HRP substrate commercial kit (Immobilon Western; Millipore Iberica) following manufacturer's instructions.

Statistical analysis

Data are given as mean ± s.e.m.. Significant differences with the control group were determined by the Student *t*-test. A *P*-value $\leqslant 0.05$ was considered significant. All data sets were analyzed using SPSS 15.0 software package (SPSS, Chicago, IL, USA).

DISCLOSURE

All the authors declared no competing interests.

ACKNOWLEDGMENTS

This study was supported by FIS (PI08-1723), FICYT (PC07-004), and Fundación Nutrición y Crecimiento. The results of this study were partially presented at the 8th symposium of the International Pediatric Nephrology Association on growth and nutrition in children with chronic renal disease, Oviedo, Spain, 2009, and at the 43rd annual scientific meeting of the European Society for Paedriatric Nephrology, Birmingham, UK. The authors gratefully thank the technical assistance of Lucía Mallada and Teresa Usín. We also thank Lourdes Tricas for her help in measuring rapamycin levels and Verdad Curto-Reyes for western blot technical support.

REFERENCES

1. Chueh SC, Kahan BD. Clinical application of sirolimus in renal transplantation: an update. *Transpl Int* 2005; **18**: 261–277.
2. Flechner SM, Goldfarb D, Modlin C *et al.* Kidney transplantation without calcineurin inhibitor drugs: a prospective, randomized trial of sirolimus versus cyclosporine. *Transplantation* 2002; **74**: 1070–1076.
3. Morales JM, Campistol JM, Kreis H *et al.* Sirolimus-based therapy with or without cyclosporine: long-term follow-up in renal transplant patients. *Transplant proc* 2005; **37**: 693–696.
4. Kahan BD, Knight R, Schoenberg L *et al.* Ten years of sirolimus therapy for human renal transplantation: the University of Texas at Houston experience. *Transplant Proc* 2003; **35**: 25s–34s.
5. Mathew T, Kreis H, Friend P. Two-year incidence of malignancy in sirolimus-treated renal transplant recipients: results from five multicenter studies. *Clin Transplant* 2004; **18**: 446–449.
6. Stallone G, Schena A, Infante B. Sirolimus for Kaposi's sarcoma in renal-transplant recipients. *N Engl J Med* 2005; **352**: 1317–1323.
7. Motzer RJ, Escudier B, Oudard S, *et al.*, for the RECORD-1 Study Group. Efficacy of everolimus in advanced renal cell carcinoma: a double-blind, randomised, placebo-controlled phase III trial. *Lancet* 2008; **372**: 449–456.
8. Bissler JJ, McCormack FX, Young LR *et al.* Sirolimus for angiomyolipoma in tuberous sclerosis complex or lymphangioleiomyomatosis. *N Engl J Med* 2008; **358**: 140–151.
9. Hay N, Sonenberg N. Upstream and downstream of mTOR. *Genes Dev* 2004; **18**: 1926–1945.
10. Guba M, von Breitenbuch P, Steinbauer M *et al.* Rapamycin inhibits primary and metastatic tumor growth by antiangiogenesis: involvement of vascular endothelial growth factor. *Nat Med* 2002; **8**: 128–135.

11. Cravedi P, Ruggenenti P, Remuzzi G. Sirolimus to replace calcineurin inhibitors? Too early yet. *Lancet* 2009; **373**: 1235–1236.
12. Ibáñez JP, Monteverde ML, Goldberg J *et al.* Sirolimus in pediatric renal transplantation. *Transplant Proc* 2005; **37**: 682–684.
13. Alvarez-Garcia O, Carbajo-Pérez E, Garcia E *et al.* Rapamycin retards growth and causes marked alterations in the growth plate of young rats. *Pediatr Nephrol* 2007; **22**: 954–961.
14. Sanchez CP, He YZ. Bone growth during rapamycin therapy in young rats. *BMC Pediatr* 2009; **9**: 3.
15. Phornphutkul C, Lee M, Voigt C *et al.* The effect of rapamycin on bone growth in rabbits. *J Orthop Res* 2009; **27**: 1157–1161.
16. Hall MN. mTOR-what does it do? *Transplant Proc* 2008; **40**: 5s–58s.
17. Rommel C, Bodine SC, Clarke BA *et al.* Mediation of IGF-1-induced skeletal myotube hypertrophy by PI(3)K/Akt/mTOR and PI(3)K/Akt/GSK3 pathways. *Nat Cell Biol* 2001; **3**: 1009–1013.
18. Starkman BG, Cravero JD, Delcarlo M *et al.* IGF-I stimulation of proteoglycan synthesis by chondrocytes requires activation of the PI 3-kinase pathway but not ERK MAPK. *Biochem J* 2005; **389**: 723–729.
19. Coolican SA, Samuel DS, Ewton DZ *et al.* The mitogenic and myogenic actions of insulin-like growth factors utilize distinct signaling pathways. *J Biol Chem* 1997; **272**: 6653–6662.
20. van der Eerden BC, Karperien M, Wit JM. Systemic and local regulation of the growth plate. *Endocr Rev* 2003; **24**: 782–801.
21. Gerber HP, Vu TH, Ryan AM *et al.* VEGF couples hypertrophic cartilage remodeling, ossification and angiogenesis during endochondral bone formation. *Nat Med* 1999; **5**: 623–628.
22. Del Bufalo D, Ciuffreda L, Trisciuoglio D *et al.* Antiangiogenic potential of the mammalian target of rapamycin inhibitor temsirolimus. *Cancer Res* 2006; **66**: 5549–5554.
23. El-Hashemite N, Walker V, Zhang H *et al.* Loss of Tsc1 or Tsc2 induces vascular endothelial growth factor production through mammalian target of rapamycin. *Cancer Res* 2003; **63**: 5173–5177.
24. Luan FL, Ding R, Sharma VK *et al.* Rapamycin is an effective inhibitor of human renal cancer metastasis. *Kidney Int* 2003; **63**: 917–926.
25. Diekmann F, Rovira J, Carreras J *et al.* Mammalian target of rapamycin inhibition halts the progression of proteinuria in a rat model of reduced renal mass. *J Am Soc Nephrol* 2007; **18**: 2653–2660.
26. Pugh CW, Ratcliffe PJ. Regulation of angiogenesis by hypoxia: role of the HIF system. *Nat Med* 2003; **9**: 677–684.
27. Le Roith D, Bondy C, Yakar S *et al.* The somatomedin hypothesis: 2001. *Endocr Rev* 2001; **22**: 53–74.
28. Kiepe D, Ciarmatori S, Hoeflich A *et al.* Insulin-like growth factor (IGF)-I stimulates cell proliferation and induces IGF binding protein (IGFB)-3 and *IGFBP-5* gene expression in cultured growth plate chondrocytes via distinct signaling pathways. *Endocrinology* 2005; **146**: 3096–3104.
29. Bohensky J, Terkhorn SP, Freeman TA *et al.* Regulation of autophagy in human and murine cartilage: hypoxia-inducible factor 2 suppresses chondrocyte autophagy. *Arthritis Rheum* 2009; **60**: 1406–1415.
30. Srinivas V, Shapiro IM. Chondrocytes embedded in the epiphyseal growth plates of long bones undergo autophagy prior to the induction of osteogenesis. *Autophagy* 2006; **2**: 215–216.
31. Ma J, Meng Y, Kwiatkowski DJ *et al.* Mammalian target of rapamycin regulates murine and human cell differentiation through STAT3/p63/Jagged/Notch cascade. *J Clin Invest* 2010; **120**: 103–114.
32. Molinos I, Santos F, Carbajo-Perez E *et al.* Catch-up growth follows an abnormal pattern in experimental renal insufficiency and growth hormone treatment normalizes it. *Kidney Int* 2006; **70**: 1955–1961.
33. Gil-Peña H, Garcia-Lopez E, Alvarez-Garcia O *et al.* Alterations of growth plate and abnormal insulin-like growth factor I metabolism in growth-retarded hypokalemic rats: effect of growth hormone treatment. *Am J Physiol Renal Physiol* 2009; **297**: 639–645.
34. Chomczynski P, Sacchi N. The single-step method of RNA isolation by acid guanidinium thiocyanate-phenol-chloroform extraction: twenty-something years on. *Nat Protoc* 2006; **1**: 581–585.